Model-independent description of the dt and d^3He systems near low-energy resonances

V. S. Popov

Institute of Theoretical and Experimental Physics, 117259 Moscow, Russia

B. M. Karnakov and V. D. Mur

Moscow Engineering-Physics Institute, 115409 Moscow, Russia

An expansion of the effective radius is employed in a model-independent description of the dt and d^3He systems in the vicinity of the low-energy ^{5}He*$(3/2^+)$ and ^{5}Li*$(3/2^+)$ resonances. The Coulomb-nuclear scattering lengths (a_{cs}) and effective radii (r_{cs}) for states with orbital angular momentum $l=0$, as well as the astrophysical function $s(E)$, are extracted from existing experimental data for the cross sections of the nuclear fusion reactions $dt \to n\alpha$ and d^3He$\to p\alpha$ in the vicinity of the resonances (data on elastic dt and $n\alpha$ scattering are also employed in the case of the dt system). Extensive use is made of the generalization of the Schwinger-Smorodinskiĭ equation for the effective radius to the case of potentials with a Coulomb barrier. A bound is established on the value of the Coulomb-nuclear effective radius $r_l^{(cs)}$ with an arbitrary value of the orbital angular momentum l, which does not depend on the specific form of the strong potential $V_s(r)$. Numerical calculations of the form factors P and Q appearing in the expansion of the effective radius are performed for different models of $V_s(r)$, and the problem of the stability of the results obtained toward possible variations of the form of the strong interaction is discussed. The analytic structure of the scattering amplitude near the elastic threshold is investigated in the presence of absorption, i.e., open reaction channels, in the system. Two series of Coulomb poles in the complex k plane, which converge near the elastic threshold $(k=0)$, are found for the dt scattering amplitude. © *1996 American Institute of Physics.* [S1063-7761(96)00111-4]

1. INTRODUCTION

The resonant nuclear reactions $dt \to n\alpha + 17.59$ MeV and d^3He$\to p\alpha + 18.35$ MeV, which have large energy releases, play an important role in nuclear physics (including thermonuclear fusion and μ catalysis), astrophysics, etc. The cross sections of these reactions in the vicinity of the s-wave ^{5}He*$(3/2^+)$ and ^{5}Li*$(3/2^+)$ resonances have been measured with extremely high accuracy,[1-4] making it possible to perform a detailed analysis of the dt and d^3He systems using an expansion of the effective radius. In these systems the resonance wave $(l=0, J^P=3/2^+)$ dominates both in elastic scattering and in the fusion reaction and largely determines the reaction cross section $\sigma_r(E)$. As was shown in Refs. 5 and 6, the elastic scattering amplitude for slow charged particles (as opposed to neutral particles) can be reconstructed, in principle, from experimental data for the reaction cross section in the region of a low-energy resonance. This makes it possible to find the Coulomb-nuclear parameters a_{cs} and r_{cs} and to perform a reliable extrapolation of the cross section $\sigma_r(E)$ to the region of small energy values $E \lesssim 10$ keV, which plays a significant role in physical applications. Direct measurement of the reaction cross section at small energies is extremely difficult because of the exponentially small permeability of the Coulomb barrier.

We use a model-independent approach, based on an expansion of the effective radius,[7-12] previously developed in the theory of systems with a Coulomb attraction potential distorted at short distances by the strong interaction (particularly in the theory of $\bar{p}p$ and $K^-\alpha$ atoms[13-15]).

As a rule, we shall henceforth use the Coulomb units $\hbar = m = a_B = 1$, where m is the reduced mass and a_B is the Bohr radius of the system.

2. LOW-ENERGY COULOMB-NUCLEAR PARAMETERS

The expansion of the effective radius for particles of like charge has the form

$$2\pi D_C(\eta)\cot\delta_{cs}(k) + 2h(\eta) = \alpha(k^2) - i\beta(k^2)$$

$$= -\frac{1}{a_{cs}} + \frac{1}{2}r_{cs}k^2 - Pr_{cs}^3k^4 + Qr_{cs}^5k^6 + \ldots, \tag{1}$$

where $l=0$, $\beta(k^2) \geq 0$ hold [from the unitarity condition, see Eqs. (4)–(6) below],

$$\alpha(k^2) = \alpha_0 + \alpha_1 k^2 + \alpha_2 k^4 + \ldots,$$

$$\beta(k^2) = \beta_0 + \beta_1 k^2 + \ldots, \tag{2}$$

$$a_{cs} = -\frac{\alpha_0 + i\beta_0}{\alpha_0^2 + \beta_0^2}, \quad r_{cs} = 2(\alpha_1 - i\beta_1),$$

$$P = -\frac{\alpha_2 - i\beta_2}{8(\alpha_1 - i\beta_1)^3}, \tag{3}$$

$\delta_{cs}(k)$, a_{cs}, and r_{cs} are the Coulomb-nuclear phase of the scattering amplitude, scattering length, and effective radius,

P and Q are the form factors, $k = \sqrt{2E}$, E is the energy in the center-of-mass system, $\eta = 1/ka_B$ is the Sommerfeld parameter,

$$D_C(\eta) = (e^{2\pi\eta} - 1)^{-1}, \quad h(\eta) = \text{Re } \psi(i\eta) - \frac{1}{2} \ln \eta^2, \tag{3'}$$

$\psi(z) = \Gamma'(z)/\Gamma(z)$, $\Gamma(z)$ is the gamma function, and $D_C(\eta)$ is the permeability of the Coulomb barrier.

Since the threshold energies of the nearest open channels ($\Delta = 17.59$ and 18.35 MeV for the fusion reactions under consideration) and closed channels ($\Delta = -2.22$ and -1.46 MeV for the $t(d,pn)t$ and $^3\text{He}(d,2p)$ reactions) significantly exceed the energies of the $^5\text{He}^*$ and $^5\text{Li}^*$ resonances, the expansion of the effective radius is applicable in the resonance energy range ($E_r \sim 50$ and 200 keV, respectively, for dt and $d^3\text{He}$ scattering). Due to the presence of the open channels, i.e., absorption in the system, the low-energy parameters (3) are complex.

The resonance s wave plays the dominant role in both elastic scattering and the fusion reaction. Confining ourselves to its contribution, from the unitarity condition for the fusion reaction cross section we obtain

$$\sigma_r(E) = \frac{2\pi}{3k^2}(1 - |S_{dt}|^2) = \frac{8\pi^2}{3E} D_C(\eta)s(E), \tag{4}$$

where

$$S_{dt} = e^{2i\sigma_0} \frac{a(k) - ib_-(k)}{a(k) - ib_+(k)}, \tag{5}$$

$\sigma_0 = \arg\Gamma(1 + i\eta)$ is the Coulomb phase of the s scattering amplitude,

$$a(k) = \alpha(k^2) - 2h(\eta), \quad b_\pm(k) = \beta(k^2) \pm 2\pi D_C(\eta),$$

and $s(E)$ is the astrophysical function:

$$s(E) = \frac{\beta(k^2)}{a^2(k) + b_+^2(k)}, \quad s(0) = \frac{\beta_0}{\alpha_0^2 + \beta_0^2} \tag{6}$$

(we note that our definition of the astrophysical function differs from that used in Refs. 1 and 2; see Appendix A). Describing the experimental data in Refs. 1 and 2 by this expression, we obtain a series of sets of low-energy parameters for the dt system (see Table I; the quality of the fit is illustrated by Fig. 1). When the α_i and β_i are calculated, the results of Ref. 16 on elastic dt scattering are also included in the treatment. This, however, does not significantly alter the low-energy parameters (compare the set of parameters corresponding to $\alpha_0 = 0.238$ in Table I with the last row, which were obtained without consideration of the results in Ref. 16; the difference between the values of χ^2 is associated with the low accuracy of the elastic scattering data). It is noteworthy that we set the form factors P and Q equal to zero in (1), since their consideration is beyond the range of accuracy of the approximation used (for further details, see Appendix A). We also stress that it becomes possible to extract the low-energy parameters from experimental data on the fusion reaction cross section owing to the interference between the nuclear and Coulomb interactions.
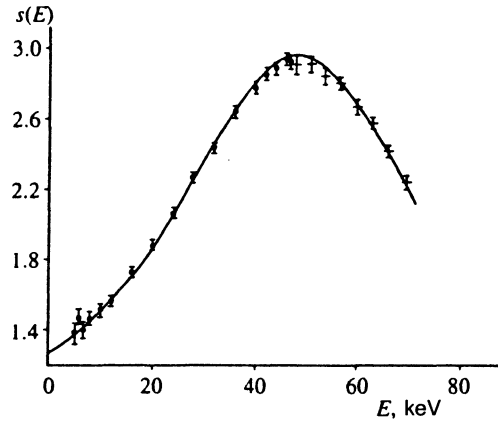

FIG. 1. The astrophysical function $s(E)$ for the fusion reaction $dt \rightarrow n\alpha$. The solid curve was calculated from Eq. (6) using the parameters in Table II; the experimental points were taken from Ref. 1 (filled circles) and from Ref. 2 (+).

As is seen from Table I, the consistent variation of all four parameters α_i and β_i ($i = 0, 1$) scarcely alters the value of χ^2 ($\chi^2 < 1$ for $0.22 < \alpha_0 < 0.32$). Therefore, additional[1] criteria are needed to select the low-energy parameters. For this purpose, we examine some properties of the effective radius r_{cs} for charged systems.

3. BOUNDS ON r_{cs} IN THE RESONANCE CASE

The effective radius r_{cs} can be expressed in terms of the real wave function[2] $\varphi_l(r) = rR_l(r, k=0)$ with zero energy:

$$r_l^{(cs)} = \frac{a_B^{1-2l}}{3(l!)^2} - 2[(2l-1)!!]^2 \int_0^\infty \left\{ \varphi_l^2 + \frac{2r\xi_l\eta_l}{a_l^{(cs)}} \right.$$
$$\left. - \frac{r^{2l+2}\eta_l^2}{[a_l^{(cs)}]^2} \right\} dr, \tag{7}$$

where

$$\xi_l(r) = \frac{\rho^{2l+1}}{2^{2l}(2l)!} K_{2l+1}(\rho),$$

$$\eta_l(r) = 2^{2l+1}(2l+1)! \rho^{-2l-1} I_{2l+1}(\rho), \tag{8}$$

TABLE I. Low-energy parameters of dt systems obtained by fitting the cross sections for $dt \rightarrow n\alpha$ fusion and elastic scattering.

α_0	α_1	$\beta_0 \cdot 10^2$	$\beta_1 \cdot 10^3$	$s(0)$	$\tilde{R}_c$	χ^2
0.20	0.1342	5.551	7.51	1.288	11.3	2.00
0.21	0.1299	6.224	6.60	1.297	10.1	1.28
0.22	0.1256	6.935	5.87	1.303	9.2	0.85
0.23	0.1212	7.681	5.41	1.306	8.4	0.66
0.238	0.1176	8.309	5.28	1.308	7.8	0.62
0.25	0.1121	9.268	5.57	1.304	6.9	0.67
0.26	0.1071	10.10	6.19	1.298	6.2	0.75
0.27	0.1017	10.97	6.98	1.292	5.6	0.82
0.28	0.0956	11.87	7.66	1.283	5.0	0.86
0.291	0.0884	12.94	7.92	1.276	4.2	0.88
0.30	0.0820	13.88	7.60	1.270	3.7	0.90
0.31	0.0745	15.01	6.55	1.265	3.2	0.95
0.32	0.0665	16.23	4.73	1.261	2.7	1.08
0.233	0.1207	7.848	7.98	1.295	8.3	0.31

with $\rho=\sqrt{8r/a_B}$ and $K_\nu(\rho)$, and $I_\nu(\rho)$ are Bessel functions of imaginary argument. The function $\varphi_l(r)$ is normalized by the asymptotic condition

$$\varphi_l(r)\approx r^{-l}\xi_l(r)-\frac{r^{l+1}}{a_l^{(cs)}}\,\eta_l(r),\quad r\gg r_N,\qquad(9)$$

so that the integral in (7) converges (here and in the following r_N denotes the characteristic radius of action of the nuclear forces). At the instant when an l level appears we have

$$a_l^{(cs)}=\infty,\quad \varphi_l(r)\equiv\chi_l(r),\qquad(10)$$

where

$$\chi_l(r)\propto\begin{cases}r^{l+1}, & r\to0,\\ r^{1/4}\exp(-\sqrt{8r/a_B}), & r\to\infty\end{cases}\qquad(10')$$

(the exponential decay of the wave function at infinity is due to the Coulomb barrier). In this case Eq. (7) is simplified significantly:

$$\tilde{r}_l^{(cs)}=2[(2l-1)!!]^2\int_0^\infty dr\left\{\left[\frac{c_l}{a_B^l}\,\xi_l(r)\right]^2-\chi_l^2(r)\right\},\qquad(11)$$

where

$$c_l=\frac{1}{2l+1}\sqrt{\frac{4l+3}{3(l!)^2(2l-1)!!}}$$

($c_0=1$, $c_1=0.509$, etc.); here and in the following quantities referring to the instant when the level appears are marked with a tilde.

We make several remarks regarding Eq. (11).

1) When the Coulomb interaction is "turned off" ($a_B\to\infty$), we have $\rho\to0$ and $\xi(0)=\eta(0)=1$, and (11) takes the form[17]

$$\tilde{r}_l^{(s)}=-2[(2l-1)!!]^2\int_0^\infty \chi_l^2(r)dr,\quad l\geq1,\qquad(12)$$

where, according to (9), the function $\chi_l(r)$ is normalized by the condition $\chi_0(r)=r^{-l}$ when $r\to\infty$.

2) As for s states, in the limit $a_B\to\infty$ the radial function $\chi_0(r)$ delocalizes, and the expression (11) transforms into the familiar formula of Schwinger[18] and Smorodinskiĭ:[19]

$$\tilde{r}_s\equiv\tilde{r}_0^{(s)}=2\int_0^\infty[1-\chi_0^2(r)]dr,\quad\lim_{r\to\infty}\chi_0(r)=1.\qquad(13)$$

3) In the case of Coulomb repulsion, the wave function of the zero-energy s state is localized at distances $r\lesssim a_B$. The expression (11) then takes the form

$$\tilde{r}_{cs}\equiv\tilde{r}_0^{(cs)}=2\int_0^\infty[\xi_0^2(r)-\chi_0^2(r)]dr$$

$$=\frac{1}{3}a_B-2\int_0^\infty\chi_0^2(r)dr,\qquad(14)$$

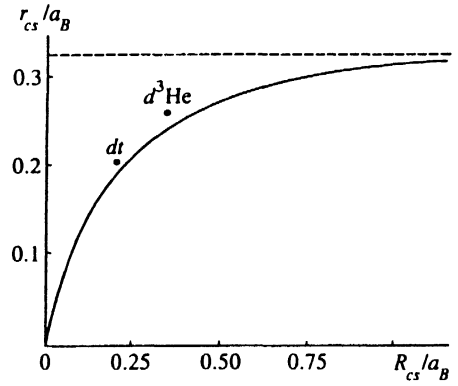which is a generalization of Eq. (13) to the case of potentials with Coulomb repulsion at large distances.

FIG. 2. Graphical representation of the inequality (17). The solid curve is a plot of the function $H_0(x_c)/3$; it corresponds to $\alpha_0=0$ and the equality sign in (15). The points for the dt and d^3He systems were calculated with consideration of the correction for incomplete binding (for the parameters presented in Table II). The dashed line corresponds to the limiting value $\tilde{r}_{cs}=a_B/3$.

Some useful bounds on the value of $\tilde{r}_l^{(cs)}$ follow from (11) and (14). Let R_c be the shortest distance at which the strong interaction begins to be negligibly small compared with the Coulomb interaction (in the R-matrix approach[20] the role of R_c is played by the charged channel radius). Since $\chi_l(r)\approx r^{-l}\xi_l(r)$ when $r>R_c$ and $\tilde{a}_l^{(cs)}=\infty$, discarding the positive term $2\int_0^\infty\chi_l^2 dr$ in (11), we arrive at the inequality

$$\tilde{r}_l^{(cs)}\leqslant\frac{a_B^{1-2l}}{3(l!)^2}H_l(\tilde{x}_c),\quad\tilde{x}_c=\frac{\tilde{R}_c}{a_B},\qquad(15)$$

where

$$H_l(x)=1-\frac{3}{2}\int_{\sqrt{8x}}^\infty K_{2l+1}^2(y)y^3 dy.$$

In particular, for an s wave

$$H_0(x)=1-\frac{1}{4}\rho^4[K_2^2(\rho)-K_1^2(\rho)]$$

$$=\begin{cases}\frac{3}{4}\left[\rho^2+\frac{1}{2}\rho^4\ln\rho+O(\rho^4)\right], & \rho\to0,\\[2mm] 1-\frac{3\pi}{8}e^{-2\rho}\left(\rho^2+\frac{7}{4}\rho\right)+\dots, & \rho\to\infty,\end{cases}\qquad(16)$$

where $\rho=\sqrt{8x}$ (Fig. 2). We stress that the bound (15) is valid for any short-range potential and for arbitrary l.

Let us demonstrate the effectiveness of the bound on $\tilde{r}_l^{(cs)}$. Table I contains several sets of low-energy parameters. They are all acceptable according to the criterion of a minimum for χ^2, the set with $\alpha_0=0.238$ corresponding to the absolute minimum of χ^2, which is equal to 0.62. However, it corresponds to the physically unacceptable value $\tilde{R}_c\approx8$ fm, which significantly exceeds the sum of the charge radii of d and t and should, therefore, be eliminated. Assuming that $R_c=5$ fm for the dt system, we can eliminate all the sets with $\alpha_0<0.26$, for which Re $r_{cs}=2\alpha_1 a_B>5.1$ fm.

In the case of exact resonance (i.e., for $1/a_{cs}=0$) the points corresponding to dt and d^3He should lie on the solid

TABLE II. Parameters of resonance Coulomb systems.

	dt	d^3He
a_B [a]	24.04	12.02
r_N	3.63	3.97
R_c	4.8	4.7
$-a_{cs}$	$76+31i$	$66+7.5i$
r_{cs}	$4.9-0.3i$	$3.5-0.2i$
P	0	$-(8.2+1.4i)\cdot10^{-2}$
$s(0)$	1.29	0.626
χ^2	0.82	0.45
E_C	59.89	239.5
C	9.107	9.113

Note. The values of a_B, r_N, R_c, and r_{cs} are given in fermis, and the values of E_c are given in kiloelectron-volts. The sum of the charge radii of the particles was taken as r_N. The coefficient C [MeV·b] appears in Eq. (A1).

curve in Fig. 2, which corresponds to the equality sign in (15). Using (7), we generalize the inequality (15) to the case of finite values of a_{cs} (see Appendix B):

$$\frac{r_{cs}}{a_B}\leq\frac{1}{3}H_0(x_c)+\alpha_0f_1(x_c)+\alpha_0^2f_2(x_c), \quad (17)$$

where

$$f_1(x)=\frac{\rho^4}{24}[I_1(\rho)K_1(\rho)+I_2(\rho)K_2(\rho)], \quad (18)$$

$$f_2(x)=\frac{\rho^4}{192}[I_1^2(\rho)-I_2^2(\rho)], $$

$x=r/a_B$, and $\rho=\sqrt{8x}$. For example, setting $\alpha_0=0.27$ and $R_c=5$ fm for the dt system, we obtain[3] $\rho=1.29$, $H_0=0.577$, $f_1=5.83(-2)$, and $f_2=8.0(-3)$, and (17) gives $r_{cs}\leq(0.192+0.016+0.001)a_B=5.01$ fm. Thus, the correction for the "incomplete binding" of the dt system[4] increases the value of r_{cs} by approximately 10%. This, in turn, corresponds to a decrease in $\tilde{R}_c$ (see Table I) by the same 10%, which was taken into account in Table II. See also Fig. 2, in which the displacement of the points for the dt and d^3He systems from the solid curve is due to consideration of the incomplete binding. We note that the value $R_c=4.8$ fm for the dt system in Table II is consistent with the choice of the charged channel radius $R_c=5$ fm used in the most recent calculations of this system within the R-matrix approach.[1,2]

It also follows from (15) and (16) that when the charges of the particles increase and $R_c\sim r_N\gg a_B$, the effective radius $\tilde{r}_{cs}$ is small (compared to r_N) and is exponentially close to its limiting value, which is equal to $a_B/3$. This can be illustrated in the examples of the Breit model (see Appendix B) and the δ potential, which allow an exact solution. In these two cases, for $\rho_c=\sqrt{8R_c/a_B}\ll1$ we obtain

$$\tilde{r}_{cs}=\frac{1}{3}a_B\left[1-d_1e^{-2\rho_c}\rho_c^2\left(1+\frac{d_2}{\rho_c}+\ldots\right)\right], \quad (19)$$

where $d_1=3\pi/8$ and $d_2=7/4$ for the Breit model and $d_1=3\pi/4$ and $d_2=3/4$ for the δ potential. Therefore, in the present case, which is realized, for example, in the $\alpha\alpha$ system,[21] Coulomb renormalization of the effective radius plays a very important role.

To conclude this section, we make two remarks.

1) In addition to the stringent upper bounds (15) and (17), we can also obtain a useful, though fairly rough, lower bound on r_{cs} [see Eq. (B5) in Appendix B].

2) The introduction of terms proportional to r_{cs}, r_{cs}^3 etc. into the expansion (1) enables us to take into account phenomenologically the effective radius of the system (its "nonpointlike character") under the condition $kr_{cs}\ll1$. This distinguishes the low-energy reactions with very light nuclei considered here, for example, from the collisions of heavy nuclei, whose description requires the introduction of model conceptions regarding the structure of the nuclei and the reaction mechanisms.

4. $n\alpha$ SCATTERING AND LOW-ENERGY PARAMETERS OF THE dt SYSTEM

The lower bound on r_{cs} can be obtained from an analysis of the elastic $n\alpha$ scattering near the threshold of the dt channel.

The $^5He^*(3/2^+)$ resonance plays a significant role both in the s wave for low-energy dt scattering and in the d wave of the $n\alpha$ system near the threshold of the $n\alpha\rightarrow dt$ reaction (i.e., for the neutron energies $E_n\approx E_{th}=22.065$ MeV). Utilizing the analyticity and unitarity conditions, as well as the T invariance of the nuclear interaction, we can express the elements of the S-matrix of such a two-channel system in terms of the low-energy parameters of the dt system:

$$S_{dt\rightarrow dt}=e^{2i\sigma_0}\frac{a(k)-ib_-(k)}{a(k)-ib_+(k)}=\tau\exp[2i(\sigma_0+\text{Re }\delta_{cs})], \quad (20)$$

$$S_{dt\rightarrow n\alpha}=S_{n\alpha\rightarrow dt}=ie^{i(\sigma_0+\varphi)}\frac{\sqrt{8\pi\beta(k^2)D_C(\eta)}}{a(k)-ib_+(k)}, \quad (20')$$

$$S_{n\alpha\rightarrow n\alpha}=\tau e^{2i\mu}=e^{2i\varphi}\begin{cases}\dfrac{a(k)-ib_-(k)}{a(k)-ib_-(k)}, & E_n>E_{th}, \\[2mm] \dfrac{A(k)+i\beta(k^2)}{A(k)-i\beta(k^2)}, & E_n<E_{th}\end{cases} \quad (20'')$$

(compare, for example, Refs. 22 and 23). Here $\sigma_0(k)$ is the Coulomb phase, and $\delta_{cs}(k)$ is the Coulomb-nuclear phase of the dt scattering amplitude, $\tau=|S_{n\alpha\rightarrow n\alpha}|$ is the inelasticity parameter $(0\leq\tau\leq1$, $\tau=1$ being below the threshold of the dt channel), $|S_{dt\rightarrow n\alpha}|=\sqrt{1-\tau^2}$, $\exp[2i\delta_2(k)]=\tau\exp(2i\mu)$, $\delta_2(k)$ is the d-wave phase shift of the elastic $n\alpha$ scattering, and

$$A(k)=\alpha(-\lambda^2)-[\lambda+2\ln\lambda+2\psi(\lambda^{-1})], \quad k=i\lambda. \quad (21)$$

Finally, φ is the phase of the potential $n\alpha$ scattering. This is the only additional parameter (beside α_i and β_i) that determines the elastic $n\alpha$ scattering in the resonance $D_{3/2}$ wave. In the energy range under consideration the phase φ can be assumed constant, its numerical value being small.[5]

It follows from (20") that

$$\mu-\varphi=\frac{1}{2}\left(\arctan\frac{b_-}{a}+\arctan\frac{b_+}{a}\right). \quad (22)$$
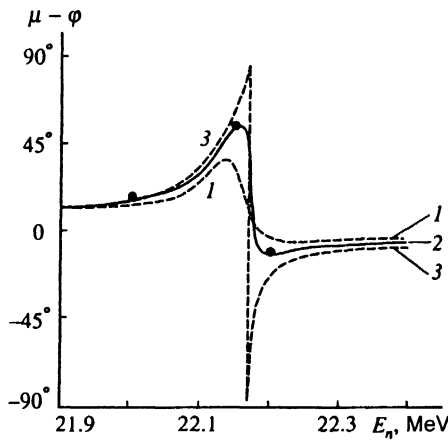
FIG. 3. Energy dependence of the phase $\mu - \varphi$ for the $D_{3/2}$ wave of elastic $n\alpha$ scattering. Curves 1, 2, and 3 correspond to the sets with $\alpha_0 = 0.238$, 0.28, and 0.32. The experimental points were taken from Ref. 24.

We note that the functions $a(k)$ and $b_-(k)$ appearing therein have zeros at resonance:

$$a(k_a) = 0, \quad 22.148 \text{ MeV} < E_n^{(a)}$$

$$b_-(k_b) = 0, \quad 22.195 \text{ MeV} > E_n^{(b)},$$

the values of the energies $E_n^{(a)}$ and $E_n^{(b)}$ being close to one another.[6] Therefore, the energy dependence of the phase shift $\mu - \varphi$ turns out to be very sensitive to the magnitude of α_0 (see Fig. 3, as well as Ref. 21). This allows us to obtain the bounded interval $0.26 \leqslant a_0 \leqslant 0.28$, which gives

$$\text{Re } a_{cs} = -76 \pm 4 \text{ fm}, \quad \text{Im } a_{cs} = -31.0 \pm 0.2 \text{ fm},$$

$$\text{Re } r_{cs} = 4.9 \pm 0.3 \text{ fm}, \quad \text{Im } r_{cs} = -0.34 \pm 0.04 \text{ fm}, \quad (23)$$

$$s(0) = 1.29 \pm 0.01.$$

The values presented are determined directly from existing experimental data and have small errors, especially $s(0)$.

Thus, taken together, the bound (15) and the phase-shift analysis data for $n\alpha$ scattering at $22.16 < E_n < 22.21$ MeV significantly reduce the uncertainty in extracting the low-energy parameters of the dt system.

Using the set of values for the low-energy parameters α_i and β_i presented above, we can calculate the astrophysical function $s(E)$ and the fusion reaction cross section at the minimal energies[7] $E \lesssim 5$ keV. The results of the calculation are shown in Fig. 4, where the solid curve corresponds to the set of data from Table I with $\alpha_0 = 0.27$, while the two dashed curves correspond to $\alpha_0 = 0.26$ and 0.28.

As is seen from Fig. 4, the experimental points in this energy range have irregular positions and are located outside the error corridor following from the bounds on $s(E)$ established above. Our calculated values of $s(E)$ have a small error ($\lesssim 1\%$), because they were obtained on the basis of the experimental data for $\sigma_r(E)$ at resonance, which have 1% accuracy. Since the data from Ref. 24 on elastic $n\alpha$ scattering near the $^5\text{He}^*$ resonance were also used in the calculations, the further increase in their accuracy at $E_n \approx E_{\text{th}} \approx 22$ MeV makes it possible to obtain a more reliable upper bound on α_0 and seems very desirable.

A similar analysis was performed for the $d^3\text{He}$ system (see Appendix B). The corresponding low-energy parameters are presented in Table II. In this case the term with the form factor P should also be taken into account in the expansion (1) (see Appendix A). The increase in the number of fitting parameters along with the insufficient accuracy of the experimental data at $E \sim E_r$ (the error $\approx 4\%$ for the cross section of the $d^3\text{He} \rightarrow p\alpha$ reaction) preclude determining the values of a_{cs} and r_{cs} with as high an accuracy as for the dt system. Therefore, the corresponding parameters in Table II should not be considered final.

Let us now compare the results obtained with the results of other investigators. The effective-radius approximation was previously used to describe the $dt \rightarrow n\alpha$ and $d^3\text{He} \rightarrow p\alpha$ reactions by Barit and Sergeev,[5] who treated the
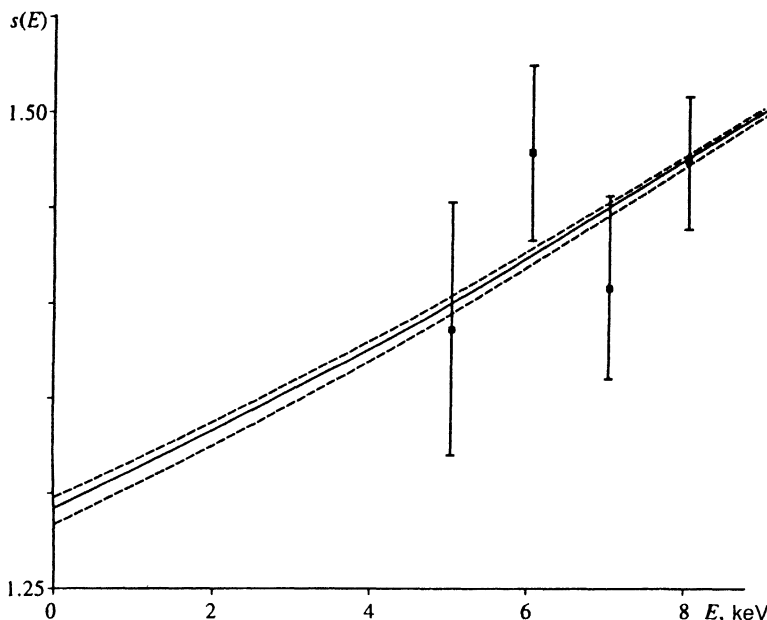

FIG. 4. Astrophysical function for the $dt \rightarrow n\alpha$ reaction at low energies. The solid curve corresponds to the set of parameters with $\alpha_0 = 0.27$, and the dashed lines correspond to $\alpha_0 = 0.26$ (upper curve) and $\alpha_0 = 0.28$ (lower line). The experimental data were taken from Ref. 1.

experimental data known at that time by varying three independent parameters, viz., Re a_{cs}, Im a_{cs}, and Re r_{cs}, and assuming Im $r_{cs}=0$. A "continuous ambiguity" was discovered in extracting the low-energy parameters (see Table I in Ref. 5), which is consistent with the data presented in Table I of this paper (selection criteria in addition to the criterion of a minimum for χ^2 were not considered in Ref. 5). Despite the considerable uncertainty in the values of the scattering lengths and the effective radius ($\sim 15\%$ for Re a_{cs} and 30% for Re r_{cs}, Barit and Sergeev[5] demonstrated the advantages of an approach based on expansion of the effective radius over the R-matrix approach in the one-level approximation, in which the charged channel radius can vary from 3 to 7 fm. In the more recent studies[1,2] this model parameter was set equal to 5 fm. However, the ambiguity associated with the choice of the number of R-matrix poles still remains. For example, the following values of the astrophysical function at zero have been given in the literature for the $dt \rightarrow n\alpha$ reaction: $s(0) = 1.272 \pm 0.007$, 1.257, and 1.285 for one-level,[1] two-level, and multilevel[2] fits, respectively.

The dt system was also considered within the resonance coupled channel model in Ref. 25. Conversion of the parameters obtained therein to the scattering length and the effective radius give values of α_i and β_i that are close to the set with $\alpha_0 = 0.30$ from Table I and $s(0) = 1.299$.

The values of $s(0)$ and especially of a_{cs} and r_{cs} have a considerable spread. The additional selection criteria that we considered make it possible to reduce this uncertainty.

5. ANALYTIC STRUCTURE OF THE SCATTERING AMPLITUDE NEAR THE ELASTIC THRESHOLD

The positions of the S-matrix poles on the complex k plane (which correspond to both bound and virtual or quasistationary levels) are determined from the equation $\cot \delta_{cs}(k) = i$, which takes the following form in the effective-radius approximation:[8]

$$\lambda + 2[\psi(1 + \lambda^{-1}) + \ln \lambda] = \frac{1}{a_{cs}} + \frac{1}{2} r_{cs}\lambda^2, \tag{24}$$

where $\lambda = -ika_B$. This equation does not depend on the model of the strong (short-range) potential $V_s(r)$.

It is known[27] that in the absence of absorption, i.e., when we have Im a_{cs} = Im $r_{cs} = 0$, the S-matrix poles for potentials with a barrier are arranged symmetrically with respect to the imaginary axis in the k plane, and Im $k < 0$. When there are open channels, the nuclear interaction breaks this symmetry and displaces the Coulomb poles away from the negative imaginary semiaxis ($k_n = -i/na_B$ for a "purely Coulomb" repulsive potential, where $n = 1, 2, \ldots$). In case of resonance, in which $|a_{cs}| \gg r_N$, there are two poles, R and R' with Im $k < 0$ close to zero. A numerical solution of Eq. (24) with the parameters presented in (23) makes it possible to obtain two additional series of Coulomb poles, $k_n = -i/\nu_n$, which crowd together near the elastic threshold $k = 0$, along with them. In the limit $n \gg 1$, for the poles in the right-hand half-plane (Re $k > 0$) we have

$$\nu_n = n + \nu_\infty - \frac{c_1}{(n + \nu_\infty)^2} + \frac{c_2}{(n + \nu_\infty)^4} + \ldots, \tag{25}$$

TABLE III. Positions of the poles of the dt scattering amplitude near the elastic threshold.

n [a]	ka_B		$\nu_n - n$	
0	$1.334 - 0.468i$	$-1.659 - 0.0656i$	$0.223 - 0.655i$	$0.024 + 0.601i$
1	$0.293 - 0.639i$	$-0.337 - 0.681i$	$0.293 - 0.593i$	$0.179 + 0.584i$
2	$0.105 - 0.407i$	$-0.116 - 0.426i$	$0.303 - 0.594i$	$0.185 + 0.594i$
3	$0.0528 - 0.293i$	$-0.0569 - 0.303i$	$0.306 - 0.596i$	$0.185 + 0.597i$
∞	0	0	$0.308 - 0.598i$	$0.185 + 0.600i$

[a] The value $n = 0$ corresponds to the poles R (right-hand half-plane, Re $k > 0$) and R' (left-hand half-plane, Re $k < 0$), and the values $n \geq 1$ correspond to two Coulomb series of poles.

where $-1/2 < \text{Re } \nu_\infty < 1/2$,

$$\nu_\infty = \frac{1}{2\pi i} \ln(1 - 2ia), \quad c_1 = \frac{a^2(1 - b)}{12\pi^2(1 - 2ia)}, \ldots, \tag{25'}$$

$a = 2\pi a_{cs}/a_B$, and $b = 3r_{cs}/a_B$. It can be shown that the asymptotic expansion (25) has good accuracy even for $n \sim 1$. The series of Coulomb poles in the left-hand k half-plane is described by a similar expression.[6]

The positions of the poles in the k plane that correspond to the low-energy parameters of the dt system from Table II are given in Table III, which also presents the corresponding values of the variable $\nu_n - n$. It is seen from the table that, as n increases, these values rapidly reach their limiting value ν_∞, which is specified by the ratio $a_{cs}/a_B = -(\alpha_0 - i\beta_0)^{-1}$. The presence of absorption in the dt system, which breaks the symmetry between the left- and right-hand poles noted above, is especially pronounced for the imaginary parts of the resonance poles R and R'.

As n increases, the Coulomb poles k_n converge near the elastic threshold, which is essentially a special point of the scattering matrix, their residues decreasing rapidly:[28]

$$S(k) = \frac{\gamma_n}{E - E_n} + O(1), \quad E \rightarrow E_n = \frac{k_n^2}{2}, \tag{26}$$

$$\gamma_n = (-1)^n \frac{\exp(-i\pi\nu_\infty)}{(n! n^{1 + \nu_\infty})^2 a_B^2}, \quad n \gg 1. \tag{27}$$

Therefore, besides the resonance poles R and R', only the first few Coulomb poles make an appreciable contribution to the scattering amplitude. We note that the residues $\gamma_n \rightarrow 0$ when $a_B \rightarrow \infty$. Thus, the poles considered are directly related to the Coulomb interaction and vanish when it is turned off.

6. CONCLUSIONS

A model-independent approach to the investigation of the resonance low-energy scattering of charged particles has been developed using an expansion of the effective radius. It permits extrapolation of the fusion reaction cross section $\sigma_r(E)$ and the astrophysical function $s(E)$ from the resonance region to the energies $E \rightarrow 0$. The low-energy parameters a_{cs}, r_{cs}, and $s(0)$ have been calculated for the dt and d^3He systems. As is seen from Table II, the effective radius r_{cs}, unlike a_{cs}, is almost real. This is easily understood within the optical-potential model, which makes it possible to obtain the estimate Im $r_{cs}/\text{Re } r_{cs} \sim -W/U$ (see Appendix

C). The small value of the ratio $\operatorname{Im} r_{cs}/\operatorname{Re} r_{cs}$ is related to the weak coupling of the channels in dt scattering. The approach developed permits investigation of the analytic structure of the scattering amplitude (when absorption occurs in the system) near the scattering threshold, $k=0$. It can also be applied to other very light nuclei.

APPENDIX A

We offer several comments regarding the calculation of the astrophysical function $s(E)$.

a. We point out its relationship to the definition of the astrophysical function $S(E)$ in Refs. 1 and 2:

$$S(E)=e^{2\pi\eta}E\sigma_r(E)=C\frac{s(E)}{1-e^{-2\pi\eta}},\tag{A1}$$

where

$$C=4\pi^2 g E_C a_B^2,\quad g=\frac{2J+1}{(2s_1+1)(2s_2+1)}=\frac{2}{3}\tag{A2}$$

(g is the statistical weight), $E_C=Z_1 Z_2 e^2/a_B$, $a_B=\hbar^2/Z_1 Z_2 e^2 m$, $\eta=1/\sqrt{2E/E_C}$, and $Z_1 Z_2>0$.

The numerical values of E_C, a_B, and the coefficient C for the dt and $d^3\mathrm{He}$ systems are given in Table II. We note that $S(E)$ has the dimensions of MeV·b and that $s(E)$ is dimensionless.

b. At low energies we can use the expansion

$$s(E)=s_0+s_1 E+O((ka_B)^2),\tag{A3}$$

where

$$s_0\equiv s(0)=\frac{\beta_0}{\alpha_0^2+\beta_0^2},$$

$$s_1=\frac{2s_0}{\beta_0}\left\{\beta_1-\left[2(\alpha_0\alpha_1+\beta_0\beta_1)-\frac{\alpha_0}{3}\right]s_0\right\}\tag{A4}$$

[for the dt system we have $s=1.2916$ and $s_1=1.978(-2)$, if E is measured in kiloelectron-volts]. The linear approximation of the expansion (A3) at $E\leqslant 2$ keV (or $\eta\geqslant 3.9$) has an accuracy better than 0.1%; however, when $E=5$ keV, its error reaches $\sim 1\%$ and rapidly increases with increasing E.

c. In the theory of μ catalysis there is significant interest in the rate $\lambda_{Jv}=\Gamma_{Jv}/\hbar$ of the fusion reaction and the shift ΔE_{Jv} of the mesomolecular level due to the strong interaction:[29]

$$\Gamma_{0v}=|R_{0v}|^2\frac{\beta(k^2)}{a^2(k)+\beta^2(k^2)}\bigg|_{E=E_{0v}}=|R_{0v}|^2 s(E_{0v}),\tag{A5}$$

$$\Delta E_{0v}=-\frac{a(k)}{2\beta(k^2)}\bigg|_{E=E_{0v}}\Gamma_{0v}.\tag{A6}$$

In (A5) we set $\beta(k^2)\approx b_+(k)$, which was justified because of the small permeability of the Coulomb barrier. For example, $D_c\approx 5\times 10^{-6}$ holds at $E=8$ keV (see the values of E_{00} and E_{01} below). Here we have $J=0$ and $v=0$ or 1 are the total angular momentum and the vibrational quantum number of the $dt\mu$ mesomolecule, R_{0v} is the value of the wave function of the nuclear subsystem at zero (i.e., when the d and t nuclei "fuse"), and

$$E_{0v}=2\mu-\frac{m}{2}-\varepsilon_{0v},\tag{A7}$$

where ε_{0v} is the binding energy of the $dt\mu$ mesomolecule, $\mu=m_\mu(m_d+m_t)/(m_\mu+m_d+m_t)$, and $m=m_\mu m_t/(m_\mu+m_t)$. The values of R_{0v} and ε_{0v} were calculated to high accuracy in the studies of Ponomarev et al..[30,31] Using their numerical values, we have $E_{00}=7.97$ keV, $E_{01}=8.26$ keV, and $R_{00}=1.019(-4)$, and $R_{01}=9.27(-5)$. Hence for the set of parameters $\alpha_0=0.27$ (see Table I) we obtain

$$\Gamma_{00}=(9.18\pm 0.09)\cdot 10^{-3}\ \text{eV},$$

$$\Gamma_{01}=(7.63\pm 0.07)\cdot 10^{-3}\ \text{eV},\tag{A8}$$

$$\Delta E_{00}=-(10.3\pm 1.0)\cdot 10^{-3}\ \text{eV},$$

$$\Delta E_{01}=-(8.6\pm 0.9)\cdot 10^{-3}\ \text{eV}.$$

These values are consistent with the values known in the literature,[25,29] but they have a higher accuracy.

d. In performing the numerical fit for the dt system, whose results are presented in Tables I and II, we adopted the form factors $P=Q=0$ in (1). We discuss the features of this approximation.

It was shown in Ref. 8 in the case of the Yukawa, Hulthen, exponential, and Gaussian potentials that the form factors P and Q are numerically small. We carried out a more detailed investigation of this question. Using the equations presented in Ref. 8 [see Eqs. (9.14) and (9.15) in that paper], we performed a calculation of the low-energy parameters, including P and Q, for various model potentials

$$V_s(r)=-\frac{g}{2r_N^2}v\left(\frac{r}{r_N}\right),\quad \hbar=m=1\tag{A9}$$

(the calculations were performed for the resonance case, i.e., at the instant when an s level appears). It is seen from Table IV that we have $-0.05<P<0.1$. As for the next term ($\propto k^6$) in the expansion (1), we can neglect it, since 1) Q is generally several times smaller than $|P|$ (with the exception of the cases in which P is anomalously small) and 2) the corresponding term in the expansion of the effective radius has an additional small parameter of order $(kr_{cs})^2\approx 0.1$ (in the case of the dt system for the energies $E\leqslant 70$ keV, which are included in the treatment). The variation of P from -0.05 to 0.05 leads to uncertainties in the low-energy parameters that exceed the range of accuracy of the present approach, i.e.,

$$\alpha_0=0.270\pm 0.006,\quad \beta_0=0.110\pm 0.005,$$

$$s(0)=1.292\pm 0.001,$$

which justifies the choice of $P=Q=0$ for the dt system.

TABLE IV. Some parameters for short-range attraction potentials.

No.	$v(x)$	$\tilde{g}_0$	$\tilde{r}_s/R$	$\tilde{P}$	$\tilde{Q}$
1	$\exp(-x)x^{-1}$	1.67981	2.120	6.616(−2)	2.860(−2)
2	$\exp(-x^2)x^{-1}$	1.75102	1.070	−6.62(−4)	−2.76(−3)
3	$\exp(-x^4)x^{-1}$	1.64009	8.784(−1)	−1.848(−2)	−1.44(−3)
4	$\theta(1-x)x^{-1}$	1.44580	8.722(−1)	−2.684(−2)	1.45(−4)
5	$(e^x-1)^{-1}$	1	3	3.812(−2)	7.81(−3)
6	$1/\sinh x$	6.41408(−1)	3.332	2.204(−2)	2.96(−3)
7	$(x^{-1}-1)\theta(1-x)$	3.09417	6.260(−1)	−1.506(−2)	−2.42(−3)
8	$\exp(-x)$	1.44580	3.541	1.246(−2)	1.56(−3)
9	$\exp(-x^2)$	2.68400	1.435	−1.812(−2)	−9.48(−4)
10	$\exp(-x^4)$	2.89237	1.069	−2.759(−2)	5.77(−4)
11	$\theta(1-x)$	2.46740	1	−3.267(−2)	1.71(−3)
12	$x/(e^x-1)$	5.87864(−1)	4.647	4.95(−4)	−7.30(−4)
13	$x/\sinh x$	3.28504(−1)	4.856	−3.79(−3)	−7.75(−4)
14	$(1-x)\theta(1-x)$	7.83735	7.870(−1)	−2.785(−2)	5.24(−4)
15	$(e^x+1)^{-1}$	1.72057	3.783	−5.35(−3)	4.98(−4)
16	$e^{-x}(1+x)$	4.67348(−1)	4.549	4.95(−4)	−5.39(−4)
17	$e^{-x}(1+x)^{-1}$	3.66478	2.695	2.740(−2)	7.17(−3)
18	$(1-x^2)\theta(1-x)$	5.12170	8.240(−1)	−2.942(−2)	9.09(−4)
19	$1/\cosh x$	7.71586(−1)	3.652	8.31(−3)	1.08(−3)
20	$(\cosh x)^{-2}$	2	2	0	0
21	$\delta(1-x)$	1	1.333	−3.750(−2)	3.01(−3)
22	Breit model	0	2	−4.167(−2)	4.17(−3)

On the other hand, for d^3He we have $(kr_{cs})^2 \lesssim 0.5$ for $E \lesssim 400$ keV; therefore, the form factor [or α_2, see (2)] should be included in the treatment in this case.

APPENDIX B

We give the necessary explanations for the derivation of Eqs. (15) and (17). For s states Eq. (7) takes the form

$$r_{cs} = 2\int_0^\infty [u_0^2(r) - \varphi_0^2(r)]dr$$

$$= \left[\frac{1}{3}H_0(x) + \alpha_0 f_1(x) + \alpha_0^2 f_2(x)\right]a_B - \int_0^r \varphi_0^2(r)dr,$$

(B1)

where $r \geq R_c$, $x = r/a_B$, $\alpha_0 = -a_B/a_{cs}$, $\varphi_0(r)$ is the wave function with a zero energy in the potential $V_s(r) + 1/a_B r$, and $u_0(r)$ is the so-called comparison function (Ref. 7):

$$u_0(r) = \xi_0(r) - \frac{r}{a_B}\eta_0(r), \quad 0 < r < \infty,$$

(B2)

i.e., the solution of the Schrödinger equation in the absence of the strong potential $V_s(r)$, which has the same asymptotic form as $\varphi_0(r)$.

If we discard the last term in (B1) and take the minimum distance at which the strong interaction can be neglected in comparison with the Coulomb interaction as r (i.e., if we set $r = R_c$), we arrive at the inequality (17). At exact resonance (when $a_{cs} = \infty$ or $\alpha_0 = 0$) it transforms into the bound (15) on $\tilde{r}_{cs}$, so that the last two terms on the right-hand side of (17) make a correction for the incomplete binding of the system or the resonance mismatch.

This correction is especially important when R_c is calculated in the case of the d^3He system. It is seen from Fig. 5, in which the solid curve was constructed using Eq. (17) and

the dashed curve was constructed using Eq. (15) and corresponds to $\tilde{R}_c$, that consideration of the incomplete binding of the system for $\alpha_2 \lesssim 5 \times 10^{-3}$ significantly reduces the value of the radius R_c. The range $\alpha_2 = 1 \times 10^{-3}$–$3 \times 10^{-3}$ corresponds to the physically reasonable values $R_c = 5$–4.5 fm. We note that for the mirror systems under consideration $R_c(d^3\text{He}) < R_c(dt) \approx 5$ fm holds, since the Coulomb interaction is two times weaker in the dt system than in the d^3He system. The point in Fig. 5 marks the value $\alpha_2 = 2 \times 10^{-3}$ (see Table II). In addition, the limiting value[21] $\tilde{\alpha}_2 = 1/60$ is shown.

We now obtain the lower bound for r_{cs}. According to the meaning of R_c, the strong interaction vanishes at $r > R_c$, and the Coulomb interaction can be neglected in the range $0 < r < R_c$ [we make the situation somewhat rougher in the narrow region where $|V_s(r)| \approx V_C(r)$]. Therefore,

$$\frac{1}{2}\tilde{r}_{cs} \approx \int_0^{R_c} [\xi_0^2 - \chi_0^2]dr,$$

$$\int_0^{R_c} \chi_0^2 dr \equiv \int_0^{R_c} [\chi_0^2(r) - \xi_0^2(R_c) + \xi_0^2(R_c)]dr$$

$$= \xi_0^2(R_c)\left\{R_c - \int_0^\infty [1 - \bar{\chi}_0^2(r)]dr\right\},$$

(B3)

where $\bar{\chi}_0(r)$ is the wave function with $E = 0$ in the strong potential at the instant when an s level appears, which satisfies the usual boundary condition $\bar{\chi}_0(\infty) = 1$ and differs from $\chi_0(r)$ only by a scaling factor. Since

$$\int_0^{R_c} \xi_0^2 dr = \frac{1}{6}H_0(x_c)a_B, \quad \tilde{r}_s = 2\int_0^\infty (1 - \bar{\chi}_0^2)dr,$$

we obtain

$$\tilde{r}_{cs} \approx \frac{1}{3}H_0(x_c)a_B - (2R_c - \tilde{r}_s)\xi_0^2(x_c). \tag{B4}$$

Neglecting here the difference between $\tilde{r}_{cs}$ and $\tilde{r}_s$, but taking into account the correction that is linear with respect to α_0 in (17), we arrive at the lower bound

$$r_{cs} \gtrsim \left\{ \frac{1}{3}H_0(x_c) - \frac{1}{4}\left[x_c^2 - \frac{4}{3}H_0(x_c)\right]\xi_0^2(x_c) \right.$$
$$\left. + \alpha_0 f_1(x_c) \right\} a_B, \tag{B5}$$

which gives $r_{cs} > 0.16 a_B$ in the case of the dt system. As a result, from (17) and (B5) we obtain 3.8 fm$< r_{cs} <$5 fm for $R_c = 5$ fm. Similarly, for the d^3He system we find 2.8 fm$< r_{cs} <$3.5 fm.

It is noteworthy that the sign of the equality in (15) in (B4) is achieved for the Breit model, which was used to describe the NN interaction at low energies and in the theory of resonant nuclear reactions.[32] This model is specified by the boundary condition

$$r_N\varphi_0'(r_N)/\varphi_0(r_N) = -g, \tag{B6}$$

where $\varphi_0(r) \equiv 0$ holds for $0 < r < r_N$ [here $R_c \equiv r_N$ and the integral discarded in (B1) equals zero]. Also, $\tilde{r}_s = 2R_c$, and (B4) transforms into (15).

We present expansions of $\xi_0(r)$ and other functions at small and large distances. In the limit $r \to 0$ we have

$$\xi_0(r) = 1 + 2r(\ln r + C_1) + O(r^2\ln r),$$
$$\eta_0(r) = 1 + r + O(r^2), \tag{B7}$$
$$f_1(r) = \frac{8}{3}r^2 + \ldots, \quad f_2(r) = \frac{2}{3}r^3 + \ldots,$$

where $C_1 = \ln 2 - 1 + 2C = 0.848 \ldots$.

At large distances $(r \to \infty)$, it is convenient to express these functions in terms of $\rho = \sqrt{8r}$:

$$\xi_0(r) = c_0\rho^{1/2}e^{-\rho}\left(1 + \frac{3}{8\rho} + \ldots\right),$$
$$\eta_0(r) = c_0^{-1}\rho^{-3/2}e^\rho + \ldots, \tag{B8}$$
$$f_1(r) = \frac{1}{24}\rho^3 + \ldots, \quad f_2(r) = \frac{1}{128\pi}\rho^2 e^{2\rho} + \ldots,$$

where $c_0 = \sqrt{\pi/2}$. Since the functions f_1 and f_2 increase rapidly at $r \gg 1$, the inequality (17) becomes meaningless, if $R_c \gtrsim a_B$ [however, in the case of the dt and d^3He systems, the bound (17) is fully effective].

APPENDIX C

We illustrate the dependence of the low-energy scattering parameters $(a_s, r_s,$ etc.) on the depth of the strong potential in the case of a rectangular well:
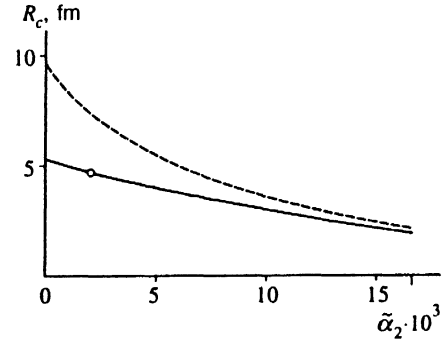
$$V_s(r) = -\frac{g}{2R^2}\theta(R - r).$$

FIG. 5. Dependence of the radius R_c on the coefficient α_2 in the expansion (2). The dashed curve corresponds to the values of $\tilde{R}_c$, and the solid curve was constructed using Eq. (17) with consideration of the incomplete binding of the d^3He system.

By matching the wave functions on the edge of the well (at $r = R$) and using the recurrence relations for Bessel functions, we find the phase of the lth scattering amplitude

$$\cot \delta_l = \frac{zN_{\nu-1}(z)J_\nu(\upsilon) - \upsilon J_{\nu-1}(\upsilon)N_\nu(z)}{zJ_{\nu-1}(z)J_\nu(\upsilon) - \upsilon J_{\nu-1}(\upsilon)J_\nu(z)}, \tag{C1}$$

where $\nu = l + 12$, $z = kR$, $\upsilon = \sqrt{z^2 + \kappa^2}$, and $g = \kappa^2$ is the dimensionless binding constant. In the case of an s wave we thus have

$$K_0(k^2) \equiv k \cot \delta_0(k) = -\frac{1}{R}\left(1 + \frac{z}{\upsilon}\tan z \tan \upsilon\right) \Bigg/$$
$$\left(\frac{\tan z}{z} - \frac{\tan \upsilon}{\upsilon}\right), \tag{C2}$$

$$a_s = \tau R, \quad r_s = \left(1 - \frac{1}{g\tau} - \frac{1}{3\tau^2}\right)R, \tag{C3}$$

$$Pr_s^3 = -\frac{1}{12}\left\{1 - \frac{3}{2g} - \frac{1}{\tau}\left[1 - \frac{3}{2g^2} - \left(\frac{3}{5} - \frac{1}{2g}\right)\frac{1}{\tau}\right.\right.$$
$$\left.\left. + \frac{1}{3\tau^2}\right]\right\}R^3, \tag{C4}$$

where $\tau = 1 - (\tan \kappa)/\kappa$ (formulas for a_s and r_s are also found in Ref. 6). At exact resonance

$$\kappa = \kappa_n = (n - 1/2)\pi, \quad n = 1, 2, \ldots,$$

$$r_s = R, \quad P = -\frac{1}{12}\left(1 - \frac{3}{2\kappa_n^2}\right).$$

We note the numerical smallness of the form factor: P varies from -0.033 for the fundamental level to -0.083 for $n \gg 1$.

In the dt and d^3He systems there is absorption caused by open reaction channels. This case can be illustrated by the model of a complex rectangular well

$$V_s(r) = -(U + iW)\theta(R - r).$$

The optical model implies $W \geq 0$. For $W = 0$ the s scattering length has poles at the points $\kappa = \kappa_n$, i.e., at the instant when

the ns level appears). Expanding (C3) and (C4) near a pole, we obtain

$$a_s = \left\{ \frac{1}{\kappa_n(\kappa - \kappa_n)} + 1 - \frac{1}{\kappa_n^2} - \left(\frac{1}{3} - \frac{1}{\kappa_n^2} \right) \frac{\kappa - \kappa_n}{\kappa_n} + \ldots \right\} R,$$
(C5)

$$r_s = \left(1 - \frac{u + iw}{\kappa_n^2} + \ldots \right) R,$$
(C6)

$$P = -\frac{1}{12} \left[1 - \frac{3}{2\kappa_n^2} - \left(1 - \frac{3}{\kappa_n^2} \right)(u + iw) + \ldots \right].$$
(C7)

Here $u = (U - U_n)/\widetilde{U}$, $w = W/\widetilde{U}$, $U_n = \kappa_n^2/2R^2$, and $\widetilde{U} = \hbar^2/mR^2$ is the characteristic depth of the short-range potential (well). We also present the expansion for the dimensionless parameter ξ:

$$\xi = \frac{1}{2\pi} \text{Im} \left(\frac{a_B}{a_s} \right) = \frac{a_B}{2\pi R} w \left[1 - 2 \left(1 - \frac{1}{\kappa_n^2} \right) u + \ldots \right],$$
(C8)

which characterizes the absorption in the system. In our case we have $\xi = \beta_0/2\pi \approx 0.02$ and 0.004 ($\beta_0 = 0.11$ and 0.025 for the dt and $d^3\text{He}$ systems, respectively). Such a small value of ξ points out the weak coupling of the reaction and elastic scattering channels.

It is seen from (C5)–(C8) that in the vicinity of resonance the real part of the scattering length varies abruptly and changes sign, while all the remaining parameters are practically constant (if the magnitude of the absorption w is fixed). The values of r_{cs} for dt and $d^3\text{He}$ are basically real (unlike a_{cs}, see Table II). A qualitative explanation for this fact is given by the estimate following from (C6)

$$\text{Im } r_s = -\frac{w}{\kappa_n^2} R + \ldots \sim -\frac{W}{U} r_N$$
(C9)

with consideration of the fact that $W \ll U$ holds at low energies.

[1])Besides the criterion of a minimum for χ^2.

[2])In this section we consider the case of arbitrary l, since the transition to $l = 0$ does not introduce any appreciable simplifications. We also neglect the absorption in the system.

[3])Here and in the following the order of magnitude of the number is indicated in parentheses, i.e., $a(-b) \equiv a \times 10^{-b}$.

[4])The conditions Re $a_{cs} < 0$ and $|\text{Re } a_{cs}| \gg r_N$ mean that even slight deepening of the strong potential $V_s(r)$ is sufficient for the appearance of a bound state in it.

[5])For example, $\varphi = 3°$, if $\alpha_0 = 0.28$ (for the values of the other parameters, see Table I).

[6])If $k_a = k_b$ holds, then we have $\tau = 0$, and the unitary limit is achieved for the $dt \to n\alpha$ reaction: $|S_{dt \to n\alpha}| = 1$. The set with $\alpha_0 = 0.291$ in Table I corresponds to this case.

[7])Direct measurements of the reaction cross sections at such low energies are hardly possible. At the same time, exact values of $\sigma_r(E)$ are of interest for thermonuclear research, especially for calculating fusion reactions in mesomolecules. We thank Yu. V. Petrov for turning our attention to the problem of extrapolating the astrophysical function into this energy range.

[8])Here we assume $Z_1 Z_2 > 0$. The case of Coulomb attraction, in which the

system has a spectrum of atomic levels that is distorted by the strong interaction at short distances ($r \lesssim r_N \ll a_B$), has been considered (on the basis of a similar equation) both for s levels[13–15] and for states with a nonzero orbital angular moment l (Ref. 26).

[1]N. J. Jarmie, R. E. Brown, and R. A. Hardekopf, Phys. Rev. C **29**, 2031 (1984).

[2]R. E. Brown, N. Jarmie, and G. M. Hale, Phys. Rev. C **35**, 1999 (1987).

[3]A. Krauss, H. W. Becker, H. P. Trautvetter, et al., Nucl. Phys. A **465**, 150 (1987).

[4]W. Möller and F. Besenbacher, Nucl. Instrum. Methods **168**, 111 (1980).

[5]I. Ya. Barit and V. A. Sergeev in Nuclear Physics and Interaction of Particles with Matter (Proceedings of the Lebedev Physics Institute, Academy of Sciences of the USSR, Vol. 44), D. V. Skobel'tsyn (ed.), Consultants Bureau, New York (1971) [Russ. original, Tr. Fiz. Inst. Akad. Nauk SSSR **44**, 3 (1969)].

[6]B. M. Karnakov, V. D. Mur, S. G. Pozdnyakov et al. Sov. Phys. JETP Lett. **51**, 399 (1990); Sov. Phys. JETP Lett. **54**, 127 (1991); Yad. Fiz. **52**, 1540 (1990) [Sov. J. Nucl. Phys. **52**, 973 (1990)] .

[7]H. A. Bethe, Phys. Rev. **76**, 38 (1949).

[8]J. D. Jackson and J. M. Blatt, Rev. Mod. Phys. **22**, 77 (1950).

[9]E. Lambert, Helv. Phys. Acta **42**, 667 (1969).

[10]B. Tromborg and J. Hamilton, Nucl. Phys. B **76**, 483 (1974).

[11]M. L. Goldberger and K. M. Watson, Collision Theory, Wiley, New York (1964).

[12]G. E. Brown and A. D. Jackson, The Nucleon-Nucleon Interaction, North-Holland (1976).

[13]A. E. Kudryavtsev and V. S. Popov, Sov. Phys. JETP Lett. **29**, 280 (1979).

[14]V. S. Popov, A. E. Kudryavtsev, and V. D. Mur, Zh. Éksp. Teor. Fiz. **77**, 1727 (1979) [Sov. Phys. JETP **50**, 865 (1979)]; Zh. Éksp. Teor. Fiz. **80**, 1271 (1981) [Sov. Phys. JETP **53**, 650 (1981)].

[15]A. E. Kudryavtsev, V. D. Mur, and V. S. Popov, Phys. Lett. B **143**, 41 (1984).

[16]Yu. G. Balashko, in Studies of Nuclear Reactions (Proceedings of the Lebedev Physics Institute, Academy of Sciences of the USSR, Vol. 33), D. V. Skobel'tsyn (ed.), Consultants Bureau, New York (1966) [Russ. original, Tr. Fiz. Inst. Akad. Nauk SSSR **33**, 66 (1965)].

[17]V. D. Mur and V. S. Popov, Teor. Mat. Fiz. **27**, 204 (1976) [Theor. Math. Phys. **27**, 429 (1977)].

[18]J. Schwinger, Phys. Rev. **72**, 742 (1947); Phys. Rev. **78**, 135 (1950).

[19]Ya. A. Smorodinskiĭ, Dokl. Akad. Nauk SSSR **60**, 217 (1948).

[20]A. Lane and R. Thomas, Rev. Mod. Phys. **30**, 257 (1958).

[21]V. D. Mur, B. M. Karnakov, S. G. Pozdnyakov et al., Yad. Fiz. **57**, 820 (1994) [Phys. At. Nucl. **57**, 769 (1994)].

[22]L. D. Landau and E. M. Lifshitz, Quantum Mechanics: Non-Relativistic Theory, 3rd ed., Pergamon Press, Oxford (1977).

[23]R. H. Dalitz, Strange Particles and Strong Interactions, Oxford University Press (1962).

[24]B. Hoop and H. H. Barschall, Nucl. Phys. **83**, 65 (1966).

[25]L. N. Bogdanova, G. M. Hale, and V. E. Markushin, Phys. Rev. C **44**, 1289 (1991).

[26]B. M. Karnakov, A. E. Kudryatsev, V. D. Mur et al., Zh. Éksp. Teor. Fiz. **94**, 65 (1988) [Sov. Phys. JETP **67**, 1333 (1988)].

[27]A. B. Migdal, A. M. Perelomov, and V. S. Popov, Yad. Fiz. **14**, 874 (1971) [Sov. J. Nucl. Phys. **14**, 488 (1972)].

[28]V. S. Popov, Preprint No. 84-90, Institute of Theoretical and Experimental Physics, Moscow (1990).

[29]B. M. Karnakov and V. D. Mur, Yad. Fiz. **44**, 1409 (1986) [Sov. J. Nucl. Phys. **44**, 916 (1986)].

[30]S. I. Vinitskiĭ, L. I. Ponomarev, I. V. Puzynin, et al., Zh. Éksp. Teor. Fiz. **74**, 849 (1978) [Sov. Phys. JETP **47**, 444 (1978)].

[31]S. I. Vinitskiĭ and L. I. Ponomarev, Elem. Chastits At. Yad. **13**, 1336 (1982).

[32]G. Breit, "Theory of resonance reactions and allied topics," in Handbuch der Physik, Vol. 41/1, S. F. Flügge (ed.), Springer-Verlag, Berlin–Göttingen–Heidelberg (1959), pp. 1–407 [Russ. transl., IL, Moscow (1961)].

Translated by P. Shelnitz